# Uranium Mineralization of Sierra Gomez, Chihuahua, Mexico

**S. M. Mitchell**
*Mobil Oil Corporation*
*Houston, Texas*

**P. C. Goodell**
**D. V. LeMone**
**N. E. Pingitore**
*University of Texas at El Paso*
*El Paso, Texas*

**Uranium and silica were leached from volcanic rock of the Mesa Formation and percolated downward to collect along the generally impermeable Cretaceous limestone. Organic matter and pyrite in the limestone furnished the reducing conditions that precipitated the uranium in a hexavalent state.**

Uranium deposits occur in Cretaceous limestone at Sierra Gomez, Chihuahua. Very few other localities are known to contain uranium in limestone. One of these, the Todilto Formation in the Grants District in New Mexico, consists of quadravalent uranium, primarily pitchblende, in organic-rich limestone. Another occurrence is the calcrete deposits of Yeelirrie, West Australia, which contain hexavalent uranium minerals syngenetically precipitated with the calcrete material. A third consists of hexavalent uranium deposits in solution channels and paleokarsts in the Madison Limestone (Mississippian) in Montana and Wyoming (Childers and Bailey, 1979). Only those deposits in the Madison Limestone appear to be analogous to those at Sierra Gomez. McEldowney and others (1977) describe mineralized zones of three types in the Madison Limestone: (1) layered uranium mineralization interbedded with silt and clay as karst fill; (2) angular fragments of country rock in clay and calcite matrix with uranium disseminated as crusts and coatings; and (3) vuggy and disseminated uranium associated with sulfides in brecciated rock.

## Aqueous Geochemistry of Uranium

Uranium normally is carried in solution in the hexavalent state and is deposited as quadravalent uranium upon entering a reducing environment, often associated with $H_2S$ or organic matter (Gabelman, 1977). Later oxidation of primary quadravalent uranium minerals may yield hexavalent minerals. Hexavalent uranium commonly is carried in solution as uranyl polycarbonate complexes. These complexes are highly soluble and mobile, explaining why uranium is not very common in limestone. Hexavalent uranium also forms aqueous uranyl fluoride complexes, which, like the carbonate complexes, are very soluble and mobile (Langmuir, 1978). Ground water may effectively leach both uranium and fluorine from ash-flow tuff of the appropriate composition, thereby mobilizing contained uranium (Waters and Granger, 1953; Zielinski, 1977, 1978, 1981; Goodell and Trentham, 1980).

The deposits at Sierra Gomez formed by leaching of uranium from ash-flow tuff by ground or geothermal waters with subsequent mobilization of that uranium as carbonate and fluoride complexes and the geochemical trapping of that uranium in a limestone host rock. The Sierra Gomez deposits thus provide insight into two growing areas of uranium research—the derivation of uranium from volcanic sources, and the deposition of uranium in limestone terranes.

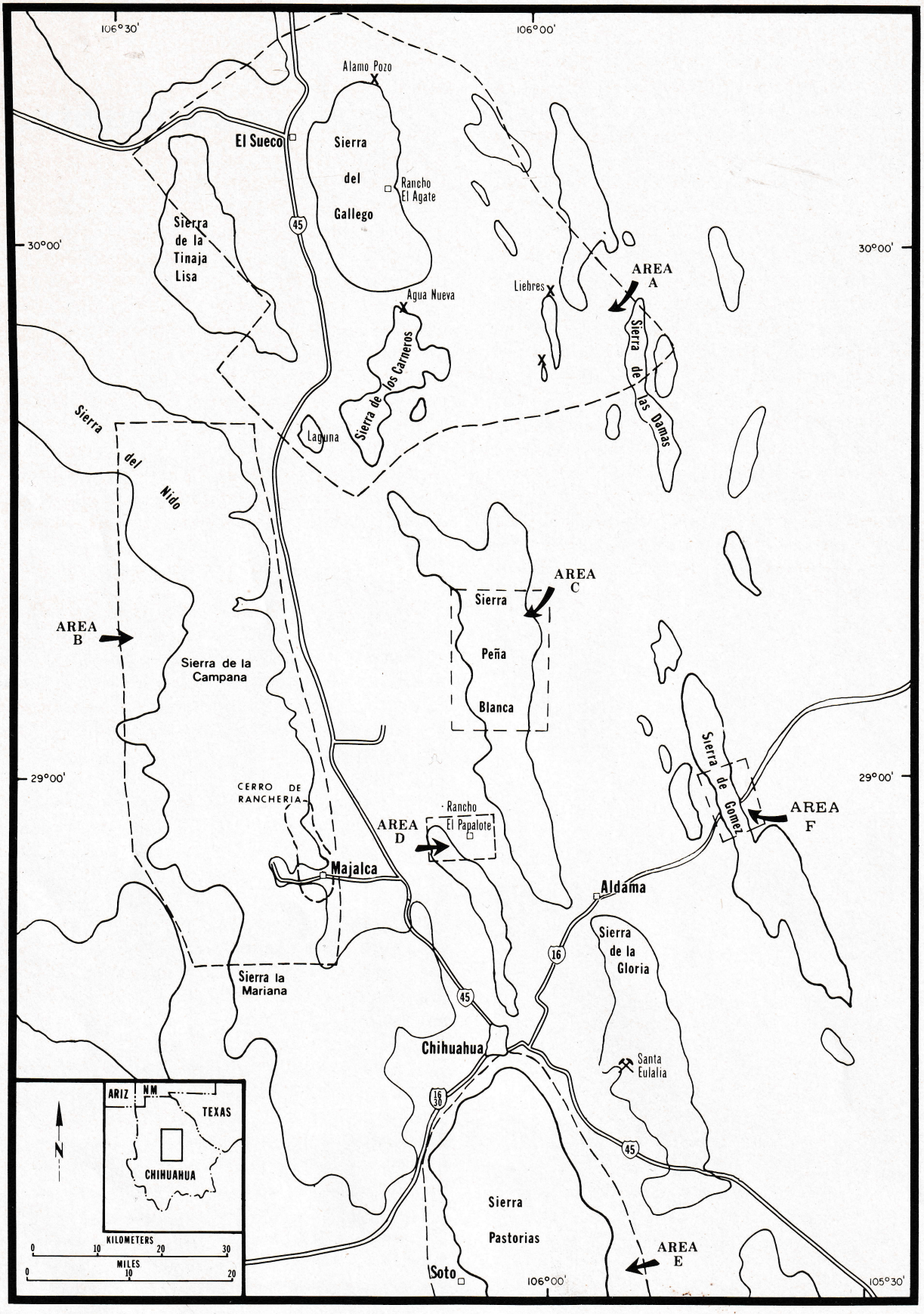



**Fig. 1**—Location of study area.

## LOCATION AND GEOLOGIC SETTING

Sierra Gomez is located approximately 50 km (30 mi) northeast of Chihuahua City, Chihuahua, Mexico (Fig. 1). The range exhibits up to 220 m (720 ft) of relief and has a maximum elevation of 1520 m (4990 ft) above sea level. Farther north, the range has higher elevations and relief, and is known as Sierra del Terreno.

Sierra Gomez is located within the Chihuahua trough, which was a negative feature during the Cretaceous. The trough was bounded on the west by the Aldama platform, 25 km (15 mi), to the west of Sierra Gomez. The Diablo platform in west Texas, on the northeast, and the Coahuila platform on the east formed the remaining known Chihuahua trough boundaries. Rudist reefs have been identified along the eastern margin of the Aldama platform in the Sierra Peña Blanca to the west of Sierra Gomez (Stege et al, 1981). This study suggests that shallow, quiet-water deposition took place at Sierra Gomez, which was probably separated from the Aldama platform to the west by deeper water.

Laramide compressional forces produced folds and thrust faults in the Cretaceous terrane. Early Tertiary exhumation resulted in local karst development. The Early Tertiary also was marked by extensive volcanism to the west, east, and south of the study area. Andesitic stratovolcanoes near the eastern boundary of the Sierra Madre Occidental were active 75 km (47 mi) to the west more than 45 m.y. ago (Mauger, 1981). This activity was followed by voluminous ash-flow tuff eruptions from 45 to 29 m.y. ago. Subsequent peralkaline tuff and flows dated at 29 m.y. are present in the Santa Clara area 75 km (45 mi) northwest of Sierra Gomez (Mauger, 1981; Dayvault, 1980; Spruill, 1980).

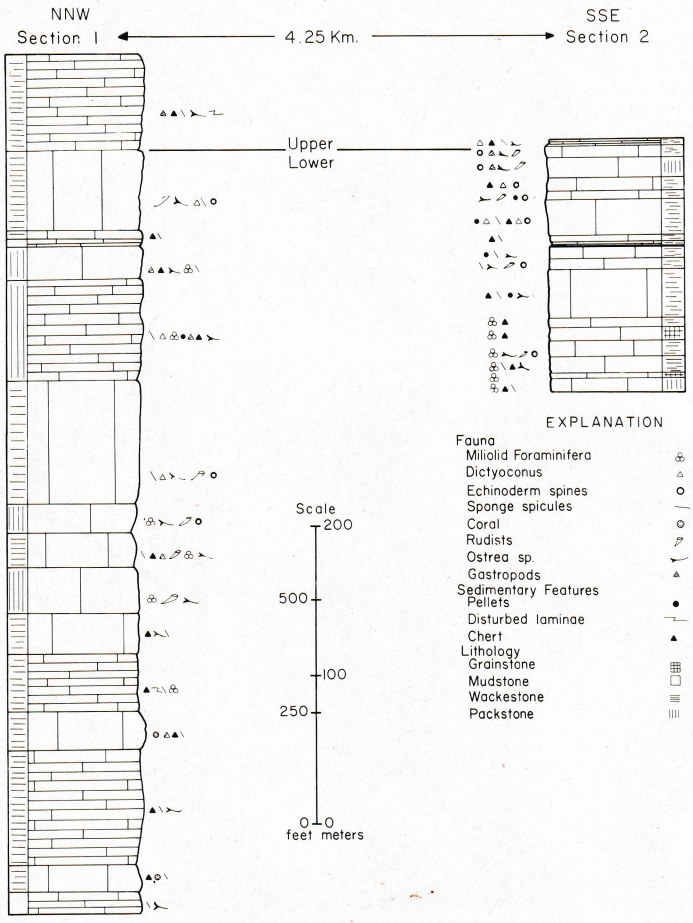



**Fig. 2**—Measured sections 1 and 2.

At Sierra Peña Blanca, 30 km (18 mi) west-northweat of Sierra Gomez, a volcanic sequence made up of five formations ranging in age from 37 to at least 44 m.y has been recognized by Alba and Chavez (1974). The uppermost unit of this sequence is the Mesa Formation, which also overlies Cretaceous limestone approximately 4 km (2.5 mi) west of Sierra Gomez. Volcanic rocks in the southern end of Sierra Gomez have not been correlated to the Peña Blanca sequence. Felsic volcanic rocks with minor intrusives of a probable age of 20 to 40 m.y. lie in a broad zone south and east of the Sierra Gomez area (McDowell and Clabaugh, 1979). Fifty km to the east of Sierra Gomez, Eocene uraninite occurs in gold-bearing, quartz-pyrite veins at Placer de Guadalupe (Krieger, 1932).

## CARBONATE STRATIGRAPHY

Approximately 500 m (1640 ft) of Middle Albian limestone is exposed at Sierra Gomez. This limestone does not directly correlate to any recognized local formation. The rocks are informally referred to as a Tamaulipas equivalent because of age correlation with the Tamaulipas Formation at Sierra Peña Blanca (Stege, 1979). The term Sierra Gomez Limestone may be used in the future.

The limestone at Sierra Gomez is informally divided into upper and lower units. The upper unit consists of approximately 61 m (200 ft) of thin bedded, laminated lime mudstone and wackestone. The lower unit includes a minimum of 440 m (1,444 ft) of interbedded massive and thin bedded mudstone, wackestone, packstone, and grainstone. Two measured sections (Fig. 2) show the units described in the area of investigation. The top of the lower unit normally consists of a highly fossiliferous, massive zone. The lower unit, in ridges on the western edge of the area, contains thick, thin-bedded intervals that grade laterally into massive limestone. The ridges in the eastern half of the area expose only a few thin-bedded intervals. At the base of the upper unit, flattened chert nodules grade in one meter vertically into continuous beds of chert and silicified limestone that weather in relief to a reddish brown color.

Pyrite occurs in many of the units, particularly in the thin-bedded intervals, which are also rich in organic material. Observed under reflected light, the pyrite commonly consists of very small cubes disseminated throughout the thin-bedded portions in both the upper and lower units. Pyrite also occurs along fractures in

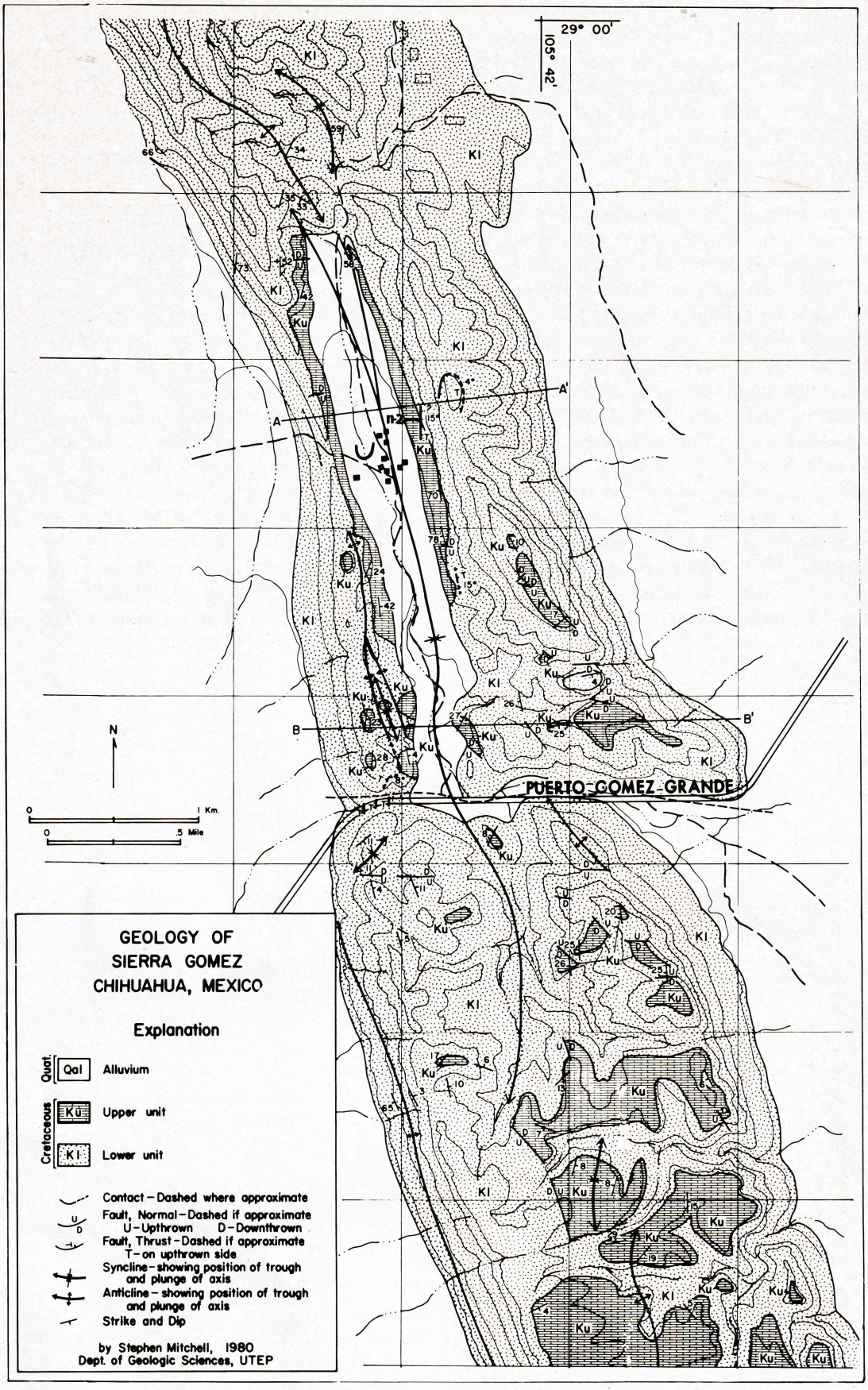



Fig. 3—Geology of Sierra Gomez, Chihuahua, Mexico.

chert from the massive units.

The carbonate sequence of Sierra Gomez is dated as Middle Albian based on the presence of the large arenaceous foraminifers *Dictyoconus walnutensis* and *Coskinolinoides texanus*. The overall aspect of the the invertebrate fauna is Fredericksburg, which is Middle and earliest Late Albian in age.

*Nummoloculina heimi, Cuneolina* sp., and several unidentified miliolid spp. have been observed in thin section. The megafauna includes sponges (borings, spicules), corals, gastropods, bivalves, serpulids, and echinoids (spines). Algae, with the exception of sparse blue-green stromatolites, are conspicuously absent.

The relative rarity of algae with no observed dasycladaceans suggests deep water deposition. Laminated spiculite, which also suggests basinal deposition, is exposed in roadcuts on Highway 16 at Sierra Gomez. Biostromes of requieniid and radiolitid rudists, *Ostrea* sp., and colonial corals, however, provide important indications of shallow water deposition. Abundant benthonic foraminifera and an absence of a pelagic fauna (ammonites and planktonic foraminifera) also suggest shallow water deposition. A stromatolitic bed exhibits typical fenestrate structure. Pre-tectonic brecciation of units 7 through 12 in measured section 2 could indicate periods of subaerial exposure resulting in solution collapse.

The limestone at Sierra Gomez indicates deposition in shallow, normal marine water with periods of subaerial exposure. The units were separated from the Aldama platform by the basinal Tamaulipas Formation. An offshore carbonate bank or platform is therefore postulated. This bank or platform may have been completely surrounded by basinal deposits.

## STRUCTURAL FEATURES

The structural configuration of the Sierra Gomez area is shown on the geologic map (Fig. 3) and vertical sections (Fig. 4). The geologic units have been both folded the thrusted. A north to south trending asymmetric syncline bounded by steep anticlinal structures crosses the core of the area. Small scale folding, which may have originated from larger scale folding of thin bedded units occurs throughout the area.

Thrust faults are observed on both sides of the north-south synclinal valley. Although we could not precisely measure displacements along the exposed faults, lithologies suggest displacements of less than 10 m.

A thrust fault, entirely in massive units, occurs in mine workings and test pits along the eastern edge of

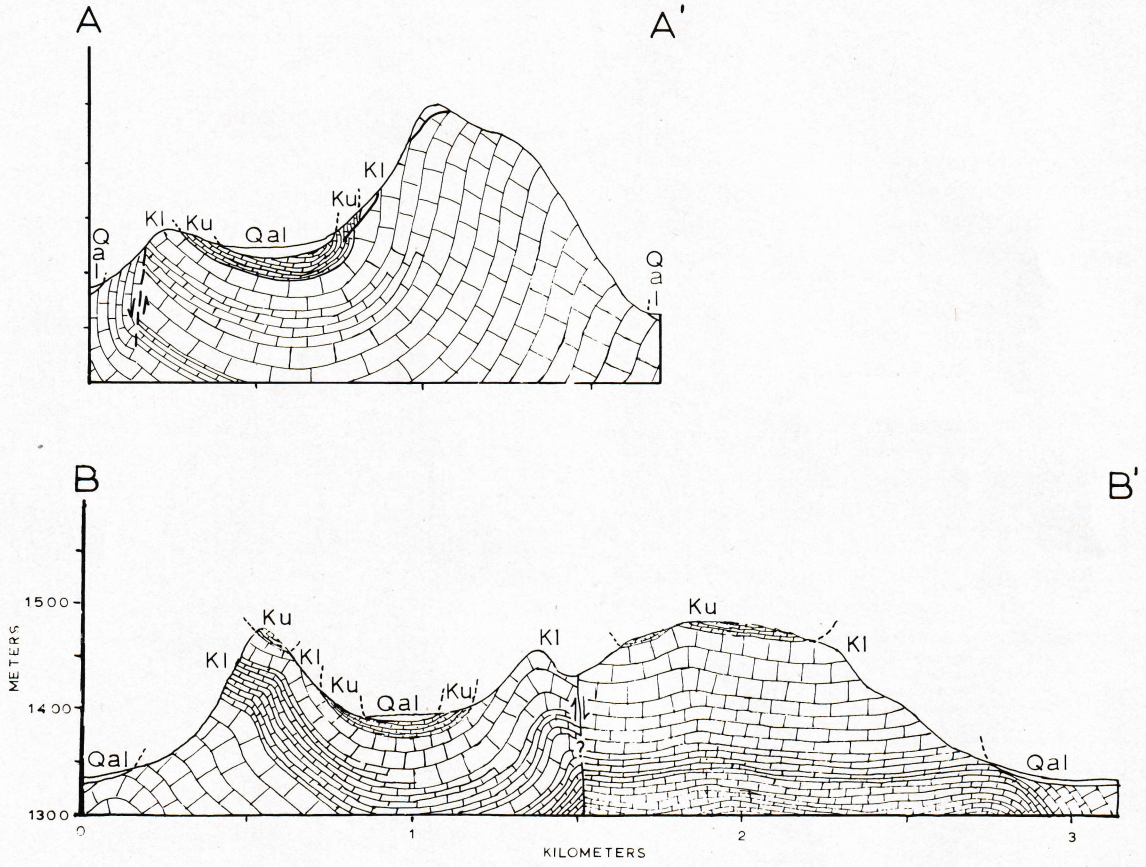



**Fig. 4**—Structural cross sections A-A′ and B-B′.

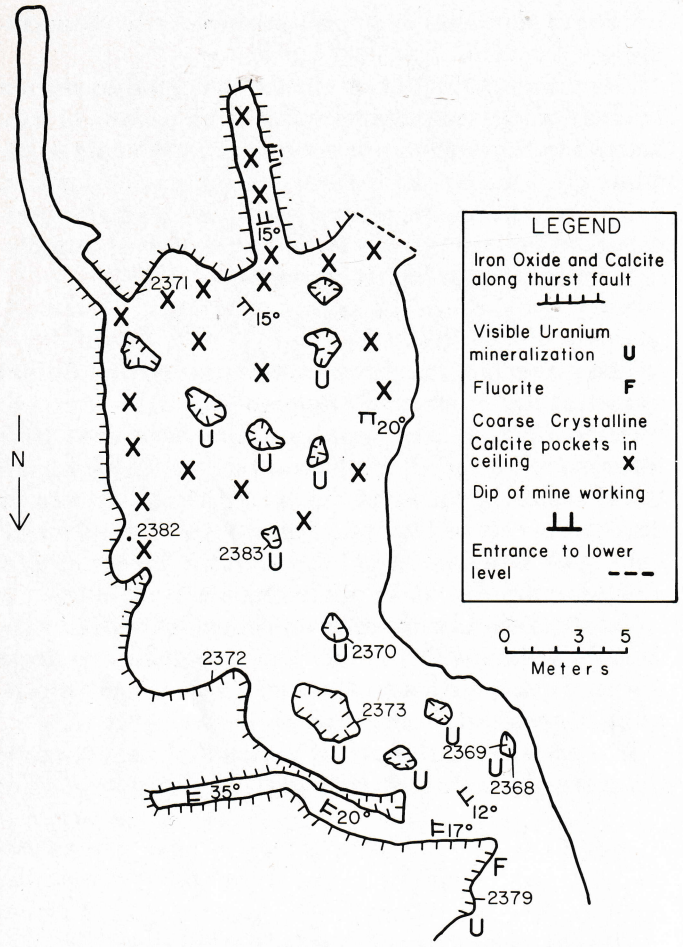



**Fig. 5**—Map of underground workings, location N-2.

the area, where it provides important sites for mineralization. It dips 4°W at the top of the eastern ridge in the area. This dip increases to the west toward the center of the syncline and at lower elevations. Near the valley floor, several visible fault planes dip 15°W. The thrust fault can be traced nearly continuously from the top of the ridge westward down the east flank of the syncline.

High angle normal faults with vertical displacements of only a few meters occur in two groups trending east to west and northwest. The east to west faults, found from 1 km north to 1 km south of highway 16, may be related to a major fault along Highway 16 through Puerto Gomez Grande. This larger fault is indicated by the sharp change in structure south of the highway. Small faults trending northwest are abundant within the area.

The folding and thrusting of the limestone apparently resulted from east-west compression. In the El Cuervo area of the Peña Blanca range, 45 km (28 mi) northwest of the Sierra Gomez, Tertiary (?) ignibrite covers Cretaceous carbonates that were involved in the earlier folding and thrusting. The compression in the region is assumed to be Laramide in age (Gries and Haenggi, 1970). Later, tension associated with Basin and Range tectonic activity resulted in the normal faults that produced the present horst and graben structure of the area. The Tertiary ignimbrite was erupted during the early phases of this tectonic activity.

## MINERALIZATION

### Mineralogy

*Uranium*–Early investigations of the mineralization at Sierra Gomez are limited to remarks by Gabelman and Krusiewski (1967), Goodell and others (1979), and unpublished reports by INEN (Instituto Nacional de Energia Nuclear). Only hexavalent uranium minerals occur at Sierra Gomez. Carnotite and metatyuyamunite were identifed by x-ray diffraction. Uranophane, identified by its acicular habit, was noted in thin sections in calcite (Plate 1C). Uranium minerals commonly occur in fracture zones and in breccia as coatings and open-space fillings, closely associated with ferric oxide. Uranium minerals also form pseudodendritic growths in chalcedony.

*Calcite*–Many varieties of calcite are present:

(1) White calcite with cleavage planes three to five inches on edge forms large masses, which, in places, constitute mappable features. The upper plate of the mineralized thrust fault in massive limestone locally contains large zones of this material (Fig. 5);

(2) travertine, commonly stalactitic, occurs as banded coarsely crystalline calcite of a dark yellowish-orange color;

(3) travertine also forms consistent bands, most of which are white;

(4) coarse yellowish-green crystalline calcite of a yellowish-green color, due to the inclusion of garnierite and tyuyamenite.

(5) white, microcrystalline calcite replacing limestone in breccia, with hexavalent uranium minerals coating cleavage planes at several locations, and associated inclusions of purple fluorite; and,

(6) grayish-black calcite, of limited distribution.

Types 4 and 5 are associated with uranium mineralization.

*Pyrite*–Sedimentary pyrite is found in limestone that is rich in organic material. Pyrite crystals up to 3 mm across occur in the fine grained calcite and clastic material that cement collapse breccia. Most commonly, however, pyrite has been oxidized to reddish or brownish ferric oxide. Iron enrichment is commonly associated with the silicification of collapse breccia. Ferric oxide invariably accompanies uranium mineralization.

*Silica*–Abundant chalcedony is present at Sierra Gomez. The introduction of quartz and hematite and other iron oxides is associated with the destruction of most or all of the primary limestone textures. Yellow chalcedony containing inclusions of hexavalent uranium minerals and garnierite cements silicified and iron enriched breccia. Chrysoprase is present and derives its color from the inclusions of garnierite and, at times, tyuy-

amunite.

*Fluorite*–Purple fluorite occurs at several locations in the area, most commonly filling fractures in massive limestone or calcite. It sometimes forms microcrystalline intergrowths with calcite, as seen in Plate 1D. A sharp zonation of fluorite and calcite can be present. Plate 1D shows a finely laminated geopetal filling of scalenohedra of calcite. Three levels of concentration are visible in the sample. The laminated material at the base is composed of pale pink calcite with some quartz. This is succeeded by a mixture of calcite and fluorite, followed by very dusky purple microcrystalline fluorite. At least three distinct stages of fluorite precipitation are recognized in other samples. The greatest abundance of fluorite is found in the area just south of Highway 16 on the eastern slopes of the syncline.

*Selenite*–Selenite is abundant at many places. Sulfur apparently was released by the oxidation of pyrite during mineralization. Sulfate then would have reacted with calcium from the limestone to form gypsum.

*Garnierite*–Garnierite is present at several locations and is also found intermixed with both calcite and silica. Chemical analyses of calcite and quartz mixtures with included garnierite shows relatively high concentrations of Ni and Zn, and lesser concentrations of Mo, V, Fe, and Co.

## Sites of Uranium Mineralization

*Mineralization in Faults*–Several favorable environments for uranium mineralization are recognized at Sierra Gomez. The most significant of these is associated with thrust faults and paleokarsts. At several locations, extensive mine workings follow deposits along thrust faults in massive limestone (Fig. 5). Alteration along thrust faults varies greatly both in width and in position. In exposures on the ridge forming the eastern edge of the area, an alteration zone has a maximum width of 5 cm. The alteration consists of red iron oxide, white calcite veins (type 5), and traces of uranium mineralization. Lower, a zone of white, coarsely crystalline calcite (type 1) up to 0.3 m wide occurs beneath the fault plane, with uranium mineralization along fractures and cleavage planes in the calcite.

At another location, mining was done along the fault zone (see Plate 1A). Several planes of movement are visible, with an average dip of 15°W. Mineralization and iron enrichment took place in and above the plane of the fault. The mineralized zone at this locality consists of hexavalent uranium minerals lining subparallel fractures in an iron-enriched calcite zone. An undergound map of this mine is shown in Figure 5. Mine mapping recorded observations made at waist level, however certain features such as the coarse crystalline zones (type 1) have been projected onto the plane of the map. They would otherwise not have appeared. The floor of the mine follows the plane of the thrust fault, which dips 15°W. An iron enriched mineralized breccia zone from 30 to 100 cm (1 to 3 ft) thick can be seen in the pillars of the mine. Solution pockets of white, coarsely crystalline calcite (type 1) are common in the upper plate of the fault. Purple fluorite fills some fractures in the lower plate.

The contact of the mineralized zone with the unaltered limestone, as observed in one of the mine pillars and in thin section, is sharp and distinct. No other alteration or dolomitization occurs. The mineralized zone consists of fine, crystalline calcite with disseminated masses of black iron oxide and hexavalent uranium minerals cut by small veins of calcite.

*Mineralization in Paleokarsts*–The other significant deposits are associated with paleokarsts. The karst features probably developed during the Early Tertiary, before the area was covered by volcanics. Most of the paleokarsts developed at or near the top of the lower unit.

Uranium mineralization is common in silicified and iron-enriched collapse breccia. All of the following are found: breccia with fresh limestone fragments cemented by chalcedony; silicified breccia cemented with calcite; and silicified breccia cemented by chalcedony. Plate 1E shows a breccia of welded tuff and limestone fragments cemented with chalcedony.

Some collapse breccia is zoned. The inner core consists of a loosely cemented limestone collapse breccia that has been silicified and iron enriched. Surrounding this is a zone up to 5 cm (2 in) wide containing a mixture of garnierite and calcite. Separating this zone from the unaltered limestone is a thin zone of purple fluorite up to 0.5 (0.2 in) wide. Some samples show a concentration of uranium mineralization at the contact between the fluorite and the garnierite zone.

## Mineral Paragenesis

Thin sections of ore samples exhibit several stages of mineralization at Sierra Gomez. The earliest event, seen in several veins and in mineralized breccia, is iron enrichment characterized by the introduction of ferric oxide. The origin of the iron oxide may have been the oxidation of sedimentary pyrite. However, much of the iron enriched limestone contains little or no sedimentary pyrite, strongly suggesting the possiblity of the introduction or local mobilization and redeposition of iron.

Sample 2349 shows hexavalent uranium mineralization with iron oxide on limestone in a zone 1 mm wide, overlapped by calcite with fluorite inclusions. This sequence is then encrusted with another stage of uranium mineralization with iron oxide 0.2 mm thick, in turn followed by more secondary calcite. Sample 2355 shows an initial stage of calcite with uranophane. This is coated by three additional iron oxide zones separated by calcite layers less than 1 mm thick. Sample 2339 has an



**Plate 1A**—Mineralized thrust fault at location N-2. Looking southeast into workings shown in Figure 6.



**Plate 1B**—Closeup of thrust fault at site N-2.

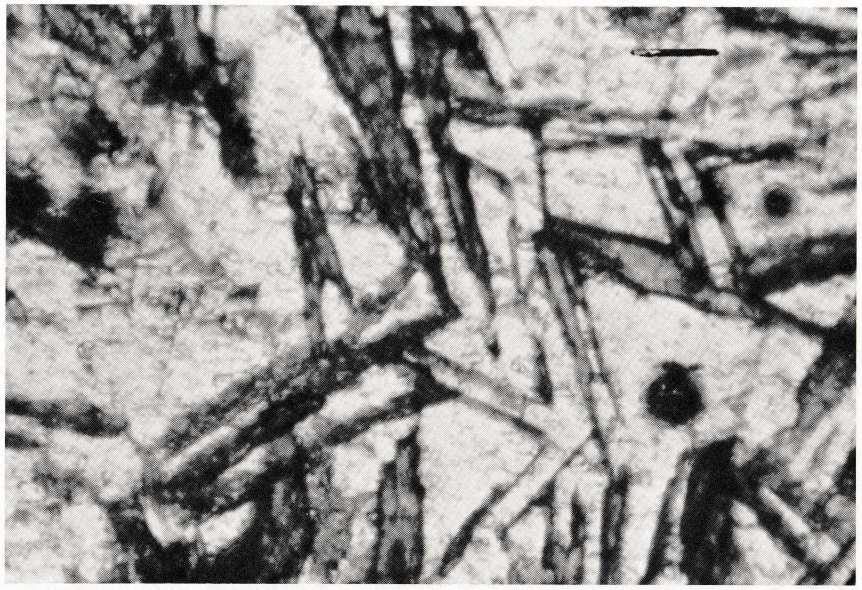


**Plate 1C**—Acicular uranophane in calcite seen in thin section.

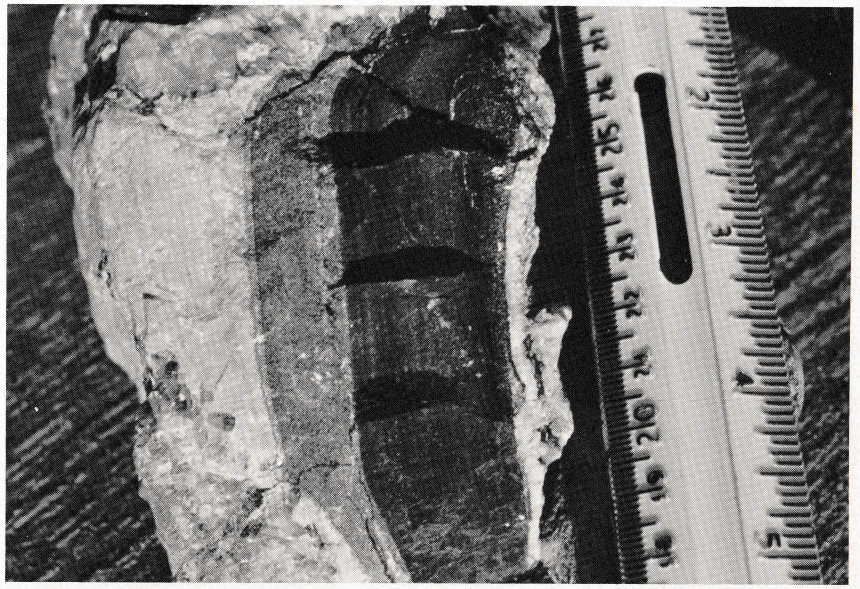


**Plate 1D**—Purple laminated microcrystalline fluorite and calcite.

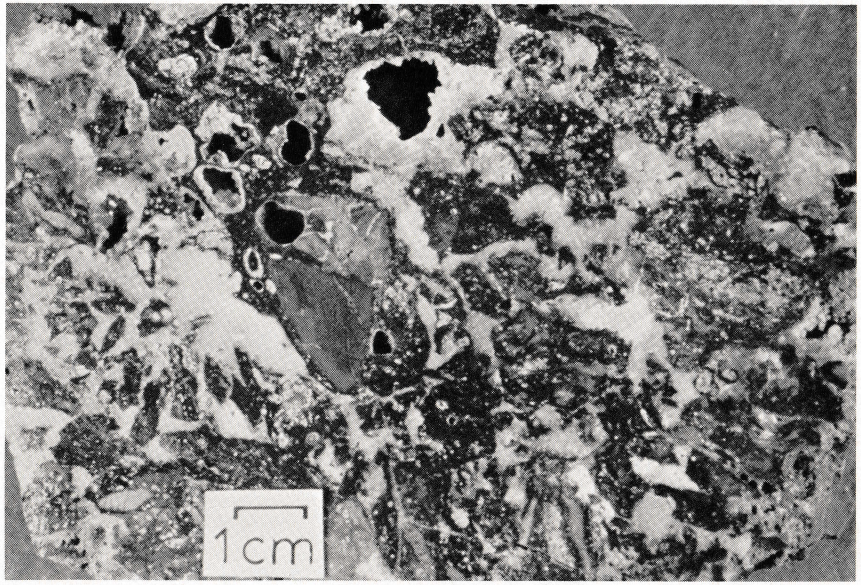



**Plate 1E**—Breccia with welded tuff and limestone fragments cemented with calcite and chalcedony containing hexavalent uranium mineral inclusion.

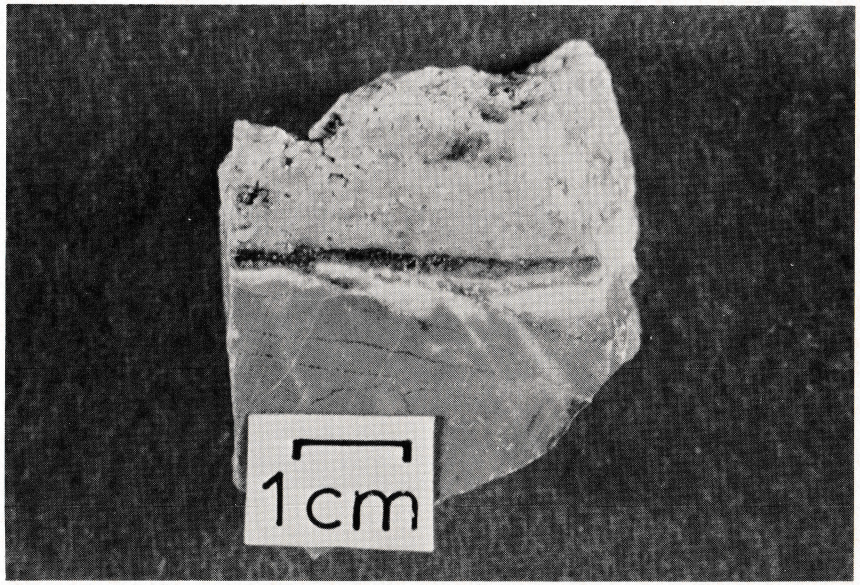



**Plate 1F**—Garnierite separated from fresh limestone by purple fluorite.

**Table 1. Trace Element Data, Sierra Gomez.**

| No. | Sample No. | Rock* Type | Element Li (ppm) | Be (ppm) | B (ppm) | Na (%) | Mg (%) | Al (%) | P (ppm) | K (%) | Ca (%) |
|---|---|---|---|---|---|---|---|---|---|---|---|
| 1 | 573 | F | 7 | <1 | <10 | <0.05 | 0.05 | 0.21 | 65 | 0.03 | 33 |
| 2 | 574 | Lms | 2 | <1 | <10 | <0.05 | 0.15 | <0.05 | 7 | <0.02 | 38 |
| 3 | 575 | F | 3 | <1 | <10 | <0.05 | 0.08 | 0.05 | 9 | <0.02 | 35 |
| 4 | 576 | M | 4 | <1 | <10 | <0.05 | 0.06 | 0.08 | <5 | 0.05 | 37 |
| 5 | 577 | M | 3 | <1 | <10 | <0.05 | 0.06 | 0.10 | 180 | 0.03 | 36 |
| 6 | 578 | G | 20 | <1 | <10 | <0.05 | 0.08 | 0.08 | 210 | 0.06 | 1.7 |
| 7 | 579 | M | 3 | <1 | 520 | <0.05 | 0.10 | 0.07 | 250 | <0.02 | 36 |
| 8 | 580 | M | 5 | 7 | <10 | <0.05 | <0.05 | <0.05 | <5 | <0.02 | 7.5 |
| 9 | 581 | Lms | 6 | <1 | <10 | <0.05 | 0.18 | 0.08 | 22 | <0.02 | 20 |
| 10 | 582 | C | 3 | <1 | <10 | <0.05 | 0.07 | 0.08 | 15 | 0.02 | 16 |
| 11 | 583 | M | 4 | <1 | <10 | <0.05 | 0.05 | 0.40 | 540 | 0.08 | 2.0 |
| 12 | 584 | Lms | 2 | <1 | <10 | <0.05 | 0.18 | <0.05 | 18 | <0.02 | 39 |
| 13 | 585 | M | 2 | <1 | 390 | <0.05 | 0.07 | 0.06 | 200 | 0.02 | 36 |
| 14 | 586 | M | 11 | <1 | <10 | <0.05 | 0.21 | 0.21 | 85 | 0.04 | 33 |
| 15 | 587 | Lms | 14 | <1 | <10 | <0.05 | 0.16 | 0.16 | 52 | 0.02 | 20 |
| 16 | Limestone[1] | | 26 | 0 | 3 | 0.037 | 4.77 | 0.43 | 175 | 0.27 | 30.45 |
| 17 | Carbonate[2] | | 5 | 0 | 20 | 0.04 | 4.70 | 0.42 | 400 | 0.27 | 30.23 |
| Detection limits | | | 1 | 1 | 10 | .05 | .05 | .05 | 5 | .02 | .05 |

*C = chalcedony, F = fluorite, G = garnierite rich, Lms = limestone, M = mineralized
[1]Rankama & Sahama, 1950
[2]Turekian & Wedepohl, 1961

| No. | Rock Type | Element Sr (ppm) | Y (ppm) | Zr (ppm) | Nb (ppm) | Mo (ppm) | Ag (ppm) | Ba (ppm) | Ce (ppm) | Th (ppm) | U (ppm) |
|---|---|---|---|---|---|---|---|---|---|---|---|
| 1 | F | 220 | 1 | 2 | 10 | 42 | <2 | 9100 | <10 | 2 | 44 |
| 2 | Lms | 550 | <1 | <2 | 13 | <4 | <2 | 22 | <10 | <2 | 3.0 |
| 3 | F | 440 | <1 | <2 | 10 | 4 | <2 | 9100 | <10 | 2 | 160 |
| 4 | M | 370 | <1 | <2 | <4 | 120 | 3 | 2200 | <10 | 270 | 25000 |
| 5 | M | 85 | 1 | <2 | <4 | 260 | <2 | 49 | <10 | 46 | 4400 |
| 6 | G | 170 | 1 | 12 | <4 | 40 | 3 | 1200 | 83 | 220 | 21000 |
| 7 | M | 210 | 4 | 16 | <4 | 30000 | <2 | 32 | 20 | 41 | 4100 |
| 8 | M | 74 | 1 | <2 | <4 | 580 | <2 | 200 | <10 | 10 | 320 |
| 9 | Lms | 820 | <1 | 2 | 6 | 27 | <2 | 11 | <10 | <2 | 12 |
| 10 | C | 150 | 1 | <2 | 7 | <4 | <2 | 100 | <10 | 3 | 39 |
| 11 | M | 78 | 1 | 12 | <4 | 37 | 2 | 1600 | 27 | 140 | 12000 |
| 12 | Lms | 700 | <1 | <2 | 11 | <4 | <2 | 2 | <10 | 3 | 10 |
| 13 | M | 190 | 3 | 12 | <4 | 22000 | <2 | 1400 | <10 | 55 | 5200 |
| 14 | M | 430 | 1 | <2 | <4 | 480 | 17 | 390 | <10 | 320 | 27000 |
| 15 | Lms | 270 | 1 | 3 | 6 | <4 | <2 | 24 | <10 | <2 | 6.0 |
| 16 | | 425 | 0 | — | — | — | 0.2 | 120 | — | 1.1 | 1.3 |
| 17 | | 610 | 30 | 19 | 0.3 | 0.4 | 0 | 10 | 11.5 | 1.7 | 2.2 |
| Detection limits | | 1 | 1 | 2 | 4 | 4 | 2 | 2 | 10 | 2 | .2 |

continued next page

Table 1. Continued.

| No. | Rock Type | Element Sc (ppm) | Ti (ppm) | V (ppm) | Cr (ppm) | Mn (ppm) | Fe (%) | Co (ppm) | Ni (ppm) | Cu (ppm) | An (ppm) |
|---|---|---|---|---|---|---|---|---|---|---|---|
| 1 | F | <1 | 28 | 370 | <1 | 21 | 0.14 | <4 | 25 | 10 | 100 |
| 2 | Lms | <1 | <10 | 22 | 1 | 91 | <0.05 | <4 | 3 | <2 | 4 |
| 3 | F | <1 | 29 | 40 | 1 | 17 | <0.05 | <4 | 6 | 2 | 26 |
| 4 | M | <1 | 13 | 4300 | <1 | 220 | 0.16 | 21 | 950 | 10 | 2100 |
| 5 | M | <1 | <10 | 850 | <1 | 160 | 0.89 | <4 | 1900 | 8 | 1900 |
| 6 | G | <1 | 63 | 4300 | <1 | 77 | 0.42 | 140 | 17000 | 54 | <2 |
| 7 | M | <1 | 12 | 430 | <1 | 180 | 1.10 | <4 | 320 | 26 | 320 |
| 8 | M | <1 | <10 | 2400 | <1 | 110 | 32 | 96 | 2800 | 10 | 1400 |
| 9 | Lms | <1 | 22 | 9 | 1 | 11 | 0.07 | <4 | 7 | 2 | <2 |
| 10 | C | <1 | 24 | 5 | 2 | 21 | <0.05 | <4 | 2 | <2 | 8 |
| 11 | M | <1 | 110 | 2300 | <1 | 37 | 1.00 | 7 | 250 | 10 | 630 |
| 12 | Lms | <1 | <10 | 20 | 1 | 10 | <0.05 | <4 | 2 | <2 | <2 |
| 13 | M | <1 | <10 | 770 | <1 | 82 | 2.00 | <4 | 270 | 21 | 250 |
| 14 | M | <1 | 20 | 20000 | <1 | 190 | 1.80 | 150 | 4600 | 33 | 3100 |
| 15 | Lms | <1 | 52 | 26 | 1 | 32 | 0.11 | <4 | 6 | 2 | 11 |
| 16 | | 0 | — | <10 | 2 | 385 | 0.40 | 0 | 0 | 20.2 | ≤50 |
| 17 | | 1 | 400 | 20 | 11 | 1100 | 0.38 | 0.1 | 20 | 4 | 20 |
| Detection limits | | 1 | 10 | 2 | 1 | 4 | .05 | 4 | 2 | 2 | 2 |

iron enriched limestone zone 7 mm wide along a vein of calcite, iron oxide and uranium minerals.

Breccia is commonly iron enriched and silicified. Sample 2341 is the only breccia with chalcedony in which limestone fragments are not silicified and enriched in iron. Hexavalent uranium mineralization in silicified breccia fragments in sample 2327 suggests that uranium mineralization accompanied silicification and iron enrichment.

Silicification of the breccia was followed by calcite cementation. Samples 2327, 2328 and 2349 are silicified breccia cemented by calcite. In samples 2341, 2342, and 2A2, chalcedony with inclusions of hexavalent uranium minerals replaces calcite.

### Chemistry of Mineralized Samples

Fifteen samples from Sierra Gomez were analyzed for 29 elements, primarily utilizing plasma-source emission spectrometry at the Oak Ridge Gaseous Diffusion Plant. Detection limits and analytic results are given in Table 1. A summary of the data by sample type is documented in Table 2. Lithologic descriptions appear in Table 3.

Three fresh limestone samples, taken from the measured sections, were analyzed. Trace-element contents for average carbonates were established by Rankama and Sahama (1950) and Turekian and Wedepohl (1961). Comparison with those published analyses indicates that the fresh limestone from Sierra Gomez is slightly enriched in U and depleted in Mg, Al, K, P, Ti, and Mn. These data reflect the lack of dolomitization in the Sierra Gomez off-shore bank depositional environment. Silt and detrital particles were not available for incorporation into the carbonate bank, thereby explaining the low Mg, Al, Ti, Cr, and Zr.

Analyses of Sierra Gomez samples show concentrations of uranium ranging from 3 ppm to 2.70 wt % (Table 1). Thorium values range from 3 to 320 ppm and increase with uranium concentration. Molybdenum concentrations of up to 2.00 wt % are present. Graphs of log vanadium and barium concentrations versus log molybdenum content show enrichment of these elements in mineralized samples. One sample with garnierite contained 1.70% nickel. Selected mineralized samples show a linear increase in cobalt versus nickel. Table 2 gives the concentration ranges of these elements in the various rock types.

Concentrations of several elements vary concordantly with uranium. Figure 6 shows log-log graphs for U versus Ni, Zn, Mo, and V. Limestone and mineralized samples are separated into two distinct groups. The fluorite rich samples fall between the mineralized samples and the fresh limestone in each of the diagrams. Fluorite precipitation appears to have been genetically related to the uranium mineralization.

In three of the graphs, the garnierite bearing sample falls within the mineralized group. The exception is the uranium versus zinc diagram, where it is distinctly separate. If log U, Zn, Ni, and V are plotted against Fe (not shown), a direct correlation is shown with enrichment in these elements. The trace elements generally increase up, to three orders of magnitude, with subse-

**Table 2. Ranges of Trace-Element Contents of Different Sample Types.***

| | Fresh Limestone (4) | Fluorite abundant (2) | Garnierite abundant (1) | Chalcedony (1) | Mineralized (7) |
|---|---|---|---|---|---|
| Li | 2-14 | 3-7 | 20 | 3 | 3-11 |
| Be | Below detection limit of 1 ppm, except one mineralized sample. | | | | |
| B | Below detection limit of 10 ppm, except two mineralized samples having 390 and 520 ppm. | | | | |
| Na | Below detection limit of 0.05 wt. %. | | | | |
| Mg | .15-.18 | .05-.08 | .08 | .07 | .05-.10 |
| Al | .05-.16 | .05-.21 | .08 | .08 | .05-.40 |
| P | 7-52 | 9-65 | 210 | 15 | 5-540 |
| K | .02 | .02-.03 | .06 | .02 | .02-.08 |
| Ca | 20-39 | 33-35 | 1.7 | 16 | 7.5-37 |
| Sc | Below detection limit of 1 ppm. | | | | |
| Ti | 10-52 | 28-29 | 63 | 24 | 10-110 |
| V | 9-26 | 40-370 | 4300 | 5 | 430-20,000 |
| Cr | Below detection limit of 1 ppm except chalcedony = 2. | | | | |
| Mn | 10-91 | 17-21 | 77 | 21 | 37-220 |
| Fe | .05-.11 | .05-.14 | .42 | .05 | .16-2.00 |
| Co | 4-7 | 4 | 140 | 4 | 4-150 |
| Ni | 2-7 | 6-25 | 17,000 | 2 | 250-4600 |
| Cu | 2-2 | 2-10 | 54 | 2 | 8-33 |
| Zn | 2-11 | 26-100 | 2 | 8 | 250-3100 |
| Sr | 270-820 | 220-440 | 170 | 150 | 78-430 |
| Y | Below or at detection limit of 1 ppm, except two mineralized samples having 3 and 4 ppm. | | | | |
| Zr | 2-3 | 2-2 | 12 | 2 | 2-16 |
| Nb | 6-11 | 10 | 4 | 7 | 4 |
| Mo | 4-27 | 4-42 | 40 | 4 | 37-30,000 |
| Ag | 2 | 2 | 3 | 2 | 17 |
| Ba | 2-24 | 9100 | 1200 | 100 | 32-2200 |
| Ce | 10 | 10 | 83 | 10 | 10-27 |
| Th | 2-3 | 2 | 220 | 3 | 41-320 |
| U | 3-12 | 44-160 | 21,000 | 39 | 4100-27,000 |

*Units same as in Table 1; numbers in parentheses are sample population; elements listed in order of increasing atomic number.

quent variations being only in the increase in iron. In other words, a plateau is reached after which only iron increases. Some maximum element contents are 3% Mo, 2% V, 1.7% Ni, and 2.7% U. Uranium mineralization also is associated with depletion in Mg, Ca, Sr, and Nb, along with slight or varied enrichment in P, Ti, Mn, Co, Cu, Zr, Ag, Ba, and Th.

## GAMMA SPECTROSCOPY STUDY

Sixty samples from Sierra Gomez were analyzed for concentrations of equivalent uranium, thorium, and potassium, utilizing gamma spectroscopy. Either 100-gram or 500-gram samples were sealed in containers, and gamma radiation was detected on either 4″ or 6″ thick Harshaw Chemical NaI-Tl activated crystals. The analyzer is a Nuclear Data series 1100/2200 pulse-height analyzer used in 128-channel mode. Twenty-two samples of fresh limestone taken from the measured sections and adjacent to mineralized zones were analyzed. Analysis of samples of fluorite and several types

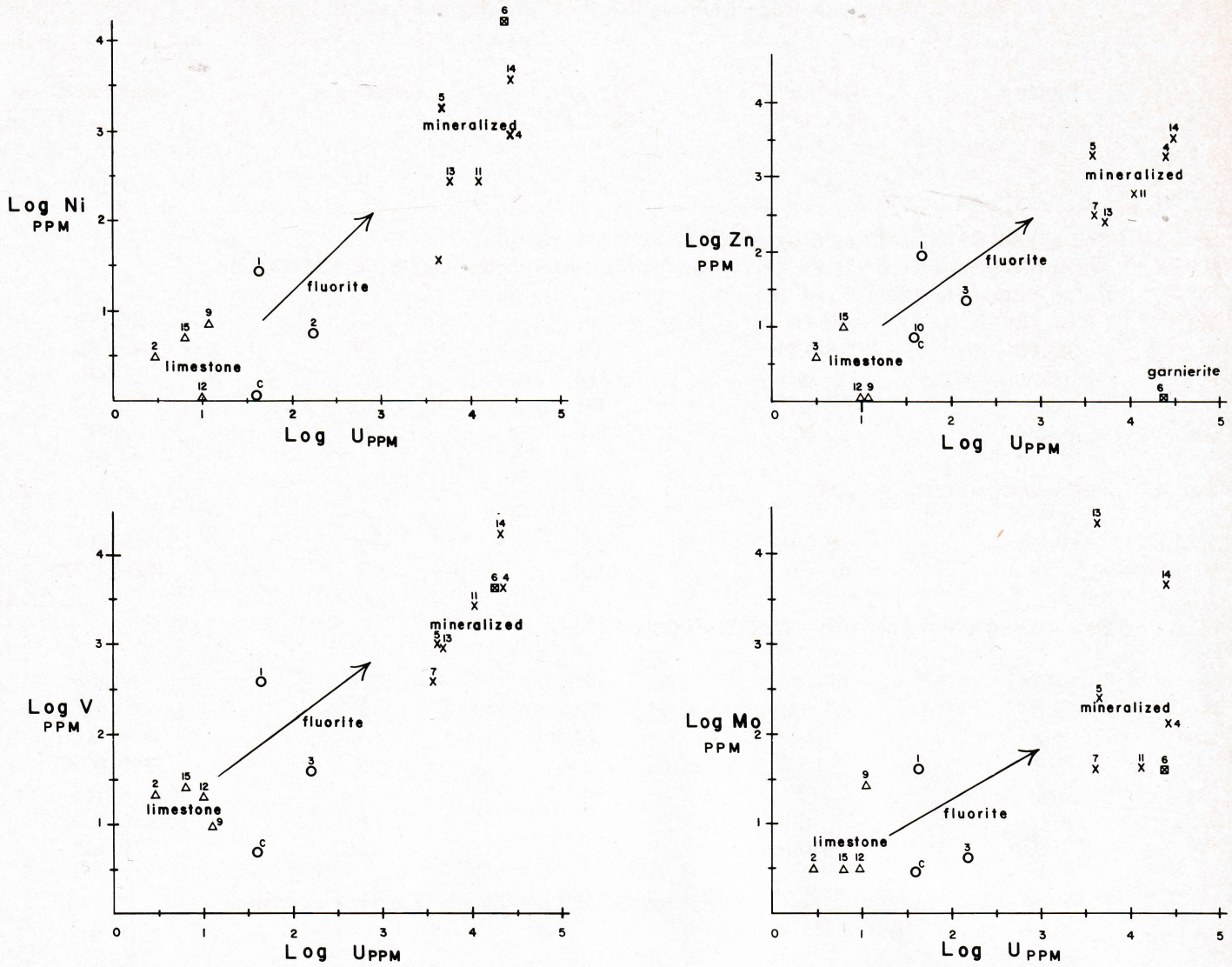



**Fig. 6**—Trace element variations correlating with uranium, Sierra Gomez, Chihuahua, Mexico.

of calcite is presented. Two samples of the Mesa Formation from 4 km (2.5 mi) west of the study area are included. Thirty-one mineralized samples were analyzed.

Thorium and potassium contents are low in most samples. However, highly mineralized samples contain up to 395 ppm Th. In addition, an antithetic relationship exists between thorium and potassium for the data set as a whole. Triangular diagrams illustrating relationship between the data by sample type are given in Figure 7.

## ORE DEPOSITION AT SIERRA GOMEZ

Three questions arise in the study of any mineral deposit. First, what was the origin or source of the ore chemicals? Second, how were these chemicals transported to the site? Third, what mechanism(s) caused the ore minerals to accumulate at that site? The answers to these questions for the uranium mineralization at Sierra Gomez constitute our mineralization model.

### Source of the Uranium

In considering possible sources of the uranium in the deposits at Sierra Gomez, it is important to establish the fact that there are no known magmatic-hydrothermal sources in the area. Gabelman and Krusiewski (1967) considered the deposits at Sierra Gomez as part of a regional zoning in response to the mesothermal deposits at the Santa Eulalia district. The relatively small, discontinuous bodies at Sierra Gomez suggest a different origin. They are quite different from the large mantos at the Santa Eulalia district, which can be traced for many km (Hewitt, 1968). Bazan (1980) believes that magmas are directly responsible for the Sierra Gomez mineralization. He postulates that a magma chamber directly underlies the area.

No evidence indicating a source at depth for the uranium bearing solutions at Sierra Gomez was identified in the present work. The virtual absence of host-rock

**Table 3. Trace-Element Sample Descriptions.**

| | Sample No. | Description |
|---|---|---|
| 1 | 573 | Geopedal structure of banded fluorite over coarse crystalline calcite; fluorite at three levels of concentration, deep purple, light purple and pink. Sample taken from the darkest purple. |
| 2 | 574 | Coarse crystalline calcite from above. |
| 3 | 575 | Highly fractured massive limestone with veins of white, coarse crystalline calcite; fractures are lined with purple fluorite. |
| 4 | 576 | Medium to fine crystalline, dark calcite with numerous fractures lined by yellow uranium minerals. One vein of white, coarse crystalline calcite cutting the specimen, without uranium mineralization. |
| 5 | 577 | Massive limestone with an altered zone made up of coarse cyrstalline calcite; reddish iron oxide, and uranium minerals lining fractures and small pocket of the altered zone. |
| 6 | 578 | Limestone replaced by silica, garnierite and tyuyamunite; trace of dark iron minerals; one cavity lined with botryoidal silica; coarse crystalline white calcite. |
| 7 | 579 | Limestone breccia with white calcite and reddish Fe-oxide cement. Uranium minerals and ferrimolybdite lining some of the iron-oxide-bearing fractures; calcite is a later filling of cavities, also forming the final cement. |
| 8 | 580 | Limestone; silicified; extreme iron enrichment, with veins of white calcite (10%); some mineralization present. |
| 9 | 581 | Massive limestone from the top of the lower unit |
| 10 | 582 | Chalcedony; white, translucent, with pockets where limestone fragments dissolved out. |
| 11 | 583 | Silicified, iron-enriched limestone with pockets of calcite cyrstals; fractures lined with uranium minerals. |
| 12 | 584 | Massive limestone near the top of the lower unit. |
| 13 | 585 | White calcite with iron oxide and calcite in fractures; with uranium minerals and ferrimolybdite lining fractures in the iron oxide-calcite mixture. |
| 14 | 586 | Massive limestone of lower unit with uranium minerals along fractures and disseminated throughout, with small masses of iron oxide. |
| 15 | 587 | Thin-bedded limestone from the upper unit. |

alteration requires low temperature mineralizing solutions. No dolomite or hydrothermal skarn has been observed in the area. The contact between mineralized limestone and unaltered limestone is normally very sharp. The only types of alteration observed are relatively thin, iron-enriched zones adjacent to veins, and calcite recrystallization.

Crucial to any hypothesis is recognition of the fact that this area was formerly overlain by volcanic rocks. The nearest extant volcanic rocks are 4 km (2.5 mi) west of the study area. These outcrops consist of two small erosional remnants of the Mesa Formation. The Mesa Formation would project to a level only a very short distance above the highest point in the Sierra Gomez area. The Mesa Formation is composed of volcanic arenite and a major ash-flow tuff. The ash-flow tuff is rhyolitic in composition, dark gray to black in color, and contains abundant pumice. Potassium-argon dating of sanidine crystals from the Mesa Formation yielded an age of 37.3± 0.7 m.y. (Alba and Chavez, 1974). The Mesa Formation contains anomalously high concentrations of U, Mo, and V. This formation also overlies the uranium deposits at Peña Blanca, and it is a probable source for the uranium throughout the region.

Devitrification of glass shards from an ash-flow tuff can release uranium and silica into solution in approximately equal pecentages (Zielinski, 1977, 1978, 1980, 1981). Zielinski's work indicates that these solutions would be highly alkaline. This condition would be similar to that found in alkaline lakes under semiarid climatic conditions.

### Uranium Transport

Two modes of aqueous transport of the uranium generated from the Mesa Formation are possible. Hexavalent uranium could be transported as either carbonate complexes or fluoride complexes–or possibly as a combination of both. Carbonate and fluoride complexes are very soluble in aqueous solutions. The uranium needed to be transported only a short distance from the Mesa Formation to the underlying Tamaulipas equivalent limestone. The primary direction of transport was

downward through the porous and permeable tuff.

### Uranium Deposition

Uranium was concentrated into commercial deposits by two mechanisms, one physical, the other chemical. The few openings (fractures, faults, and paleokarsts) in the otherwise impermeable limestone concentrated the uranium-bearing solutions in a very limited volume of the rock. There, reducing conditions caused by local organic matter and pyrite in the limestone enabled the precipitation of uranium minerals.

### Convergence of $U^{+6}$ Bearing Solutions

Once the solutions passed through the volcanic pile and reached the limestone, they were concentrated along available permeable channels. During the Laramide compression, thin bedded units folded while the more competent limestone units tended to fracture. The fractures provided permeable channels through which mineralizing solutions moved. Thrust faults and collapse breccia provided additional channels.

Figure 8 shows the hypothesized movement of mineralizing solutions. Normal faults cutting both the volcanics and the underlying limestone may have provided important pathways through which the mineralizing solutions entered the limestone. The solutions would then move along fractures, faults, and in paleokarsts until they encountered conditions favorable for precipitation. This mechanism allows the uranium generated by the leaching of the entire volume of one rock unit (the tuff) to be gathered and forced in solution through a very limited volume of another rock unit (the limestone). Paleohydrology was thus the critical mechanism in concentrating the uranium.

### Precipitation of Uranium Minerals

Mechanisms exist for the precipitation of either carbonate complexed or fluorine complexed uranium in the limestone terranes. Uranium carried as carbonate complexes would be precipitated soon after entering the limestone as a result of the reducing conditions present therein. The Sierra Gomez limestone is rich in organic matter, often emitting $H_2S$ in freshly broken pieces. In addition, the pyrite disseminated through the limestone produces reducing conditions in ground water passing through the unit. The hexavalent uranium would be reduced in this environment and precipitated. The quadravalent uranium mineral(s) would later be oxidized to the present form of the ore deposits.

In a somewhat different fashion, uranyl-fluoride com-

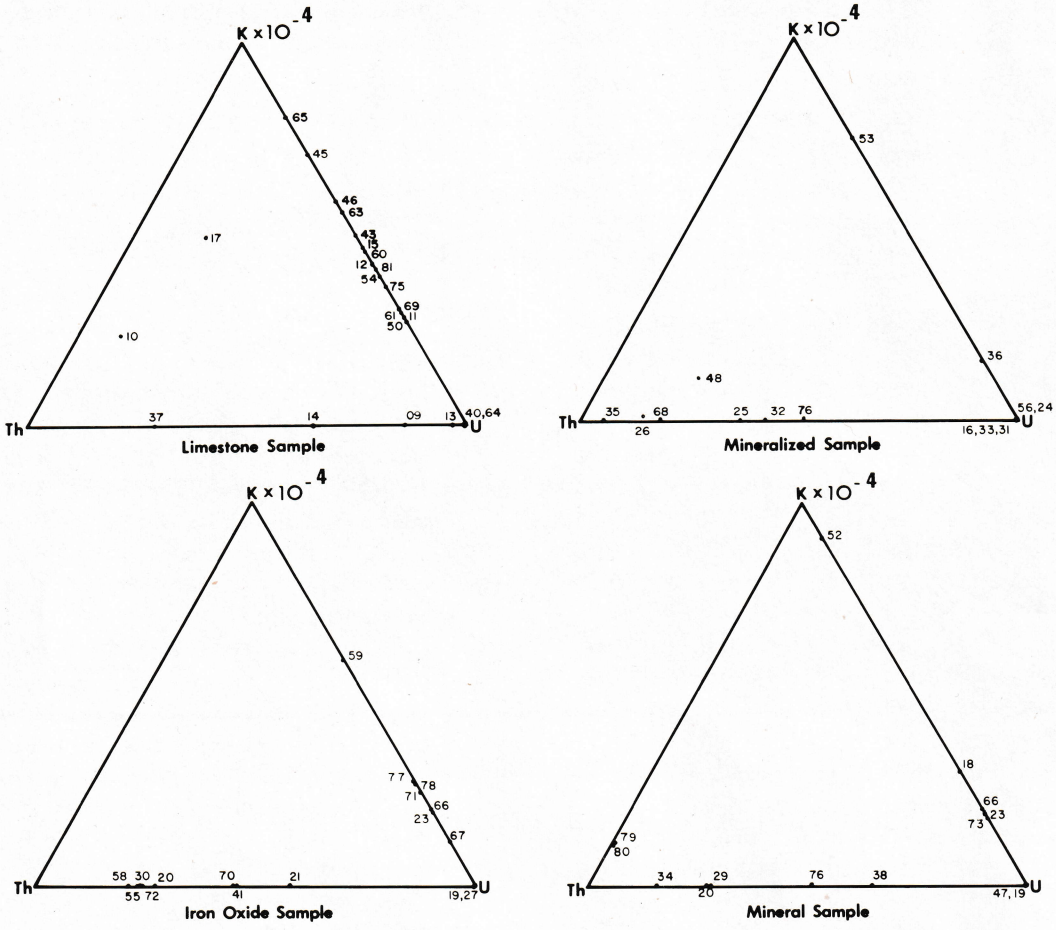



**Fig. 7**—K-U-Th contents of 60 samples from Sierra Gomez.

plexes also would undergo chemical reaction upon entering the limestone. Because the solutions initially would be low in calcium from the leaching of rhyolitic tuff, the fluorine would react with the limestone to form fluorite. This would release the uranium from the complex, resulting in an increase in the effective concentration of uranium in the solution. Precipitation of carnotite, metatyuyamunite, and uranophane would ensue. This process may explain the relationship between trace elements and uranium (Figs. 6 and 7), and the observed zonation of the collapse breccia described earlier.

As noted, hexavalent uranium minerals indicate an oxidizing environment. Abundant reddish and brownish ferric oxide at Sierra Gomez demonstrates such oxidizing conditions. This ferric oxide may have resulted from the oxidation of pyrite. Iron enrichment along faults, veins, and in paleokarsts suggests mobilization of iron under oxidizing conditions. The uranium minerals show a strong affinity for iron oxide. Plate 1B shows uranium mineralization almost surrounding large, opaque, reddish iron oxide masses.

The Eh-pH range at the time of mineralization can be estimated from the mineral assemblage present. A low temperature is assumed for reasons given earlier. Calcite, hematite, limonite, gypsum, and silica all precipitated from solutions with pH greater than 7.8. These minerals are precipitated above what Krumbein and Garrels (1952) call the iron, manganese carbonate fence with an Eh range of approximately $-1$ to $-2$, depending on the pH. These relationships are given in Figure 9. Both mechanisms of transport-precipitation (fluoride and carbonate complexes) may operate in the region bounded by the organic matter, limestone, and Fe, Mn oxide carbonate fences in Figure 9.

## CONCLUSIONS

The mineralogy, chemistry, and geologic setting of the Sierra Gomez uranium deposits indicate:

(1) Mineralization occurred in a low temperature groundwater environment. No evidence of magmatic or hydrothermal activity was encountered.

(2) Uranium rich groundwater was generated by the leaching of the overlying permeable tuff, the Mesa Formation.

(3) Uranium was carried in solution as carbonate or fluoride complexes.

(4) Solutions from the Mesa Formation flowed downward into the generally impermeable limestone along faults, fractures, and paleokarst features. This concentrated the uranium bearing solutions into a very small volume of the limestone.

(5) Uranium mineral precipitation was effected either by reducing conditions in the limestone (due to the

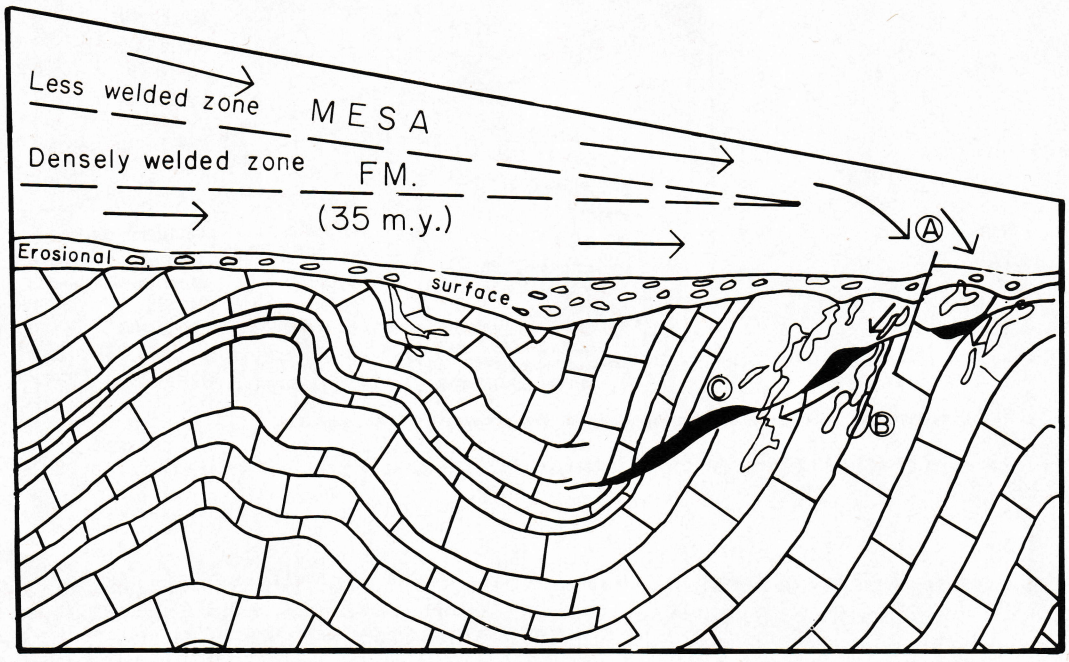



**Fig. 8**—Diagrammatic sketch of uranium mineralization, Sierra Gomez, Chihuahua, Mexico.

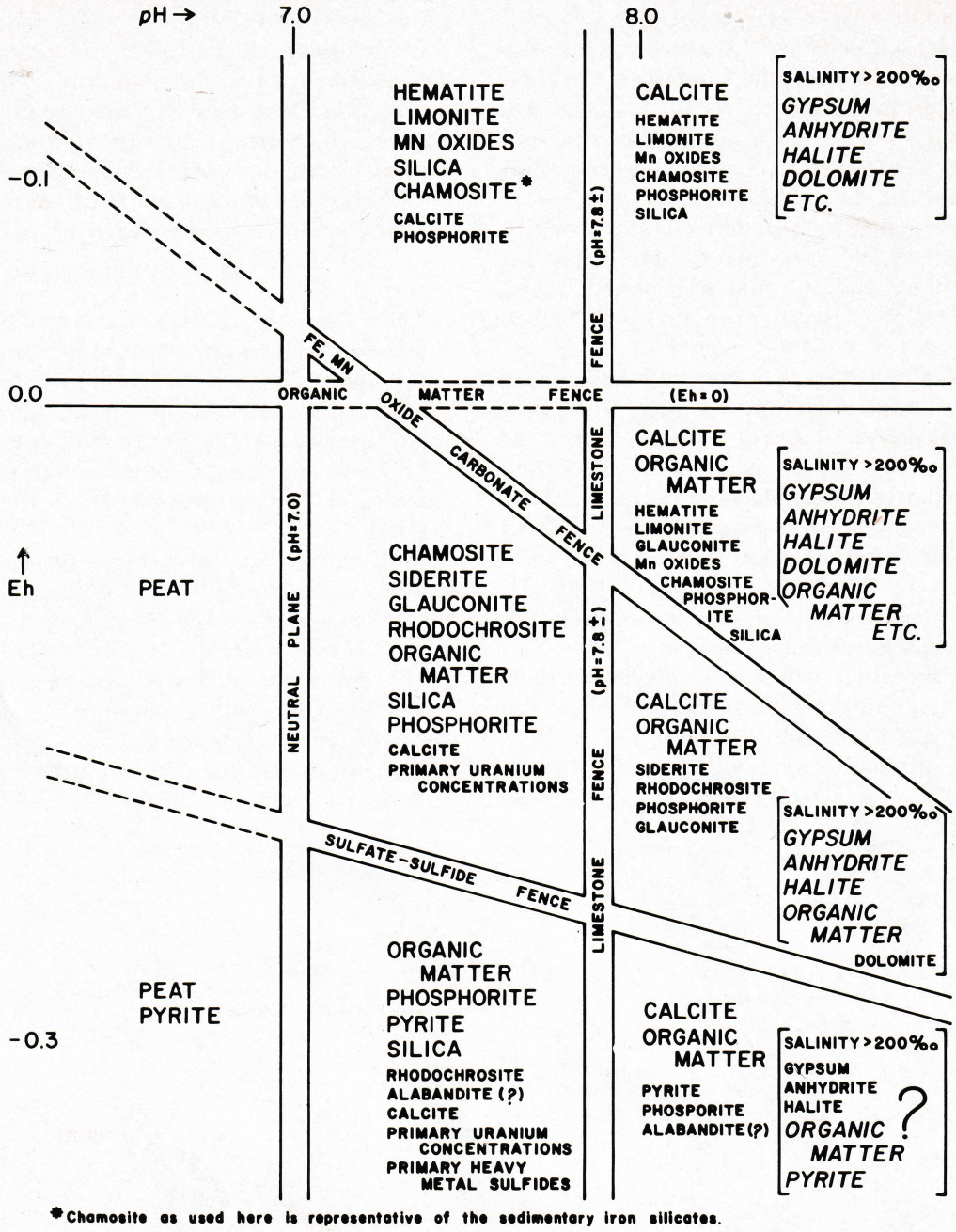



**Fig. 9**—Eh and pH controls of chemical sediments for normal seawater conditions. Brackets refer to hypersaline solutions (Krumbein and Garrels, 1952).

presence of organic matter and pyrite) or by reaction of fluoride with calcite to produce fluorite and release the uranium from its complexed state. These deposits thus illustrate both the importance of tuff as a uranium source and the viability of limestone as a host rock for uranium mineralization.

## REFERENCES CITED

Alba, L. A., and R. Chavez, 1974, K-Ar ages of volcanic rocks from the central Sierra Peña Blanca, Chihuahua, Mexico: Isochron West, no. 10, p. 21-23.

Bazan, B. S., 1980, Depositos de uranio en Faja de Tiop cordillerano: Simposium Sobre Exploration de Uranio, URAMEX, Hermosillo, Sonora, Mexico, Nov. 24.

Childers, M. D., and R. V. Bailey, 1979, Classification of uranium deposits; *in* Contributions to geology, Wyoming uranium issue II: Univ. Wyoming, v. 17, p. 188-199.

Dayvault, R. D., 1980, Peralkaline ash-flow tuffs in Santa Clara Canyon, north of Chihuahua city, Mexico: A possible source rock for uranium (abs.), *in* Abs. with Programs: Southwest Secton, AAPG Ann. Mtg., El Paso, p. 24.

Gabelman, J. W., 1977, Migration of uranium and thorium-exploration significance: AAPG Studies in Geology no. 3, 168 p.

Gabelman, J. W., and S. V. Krusiewski, 1967, Uranium deposits of Mexico: U.S. Atomic Energy Comm. RME-4099, 27 p.

Goodell, P. C., 1978, Uranium and the diagenesis in volcanic piles: NURE Geology of uranium symposium, 1977, U. S. Dept. of Energy Open File Rept., GJBX-12(78), p. 151-162.

Goodell, P. C., and R. C. Trentham, 1980, Experimental leaching of uranium from tuffaceous rocks: U. S. Dept. Energy Open-File Rept., 144 p.

——— R. C. Trentham, and K. C. Carraway, 1979, Geologic setting of the Peña Blanca uranium deposits, Chihuahua, Mexico, *in* C. D. Henry and A. Walton, eds., Formation of volcanic sediments: U.S. Dept. Energy, Open-File Rept., GJBX-22(79), p. IX1-IX38.

Gries, J. C., and W. T. Haenggi, 1970, Structural evolution of the eastern Chihuahua tectonic belt, *in* Geologic framework of the Chihuahua tectonic belt: West Texas Geol. Soc. Pub. 71-59, p. 119-137.

Hewitt, W. P., 1968, Geology and mineralization of the main mineral zone of the Santa Eulalia district, Chihuahua, Mexico: Soc. Mining Engineers Trans. 241, June, p. 228-260.

Krieger, P., 1932, An association of gold and uraninite from Chihuahua, Mexico: Econ. Geol., v. 27, p. 651-660.

Krumbein, W. C., and R. M. Garrels, 1952, Origin and classification of chemical sediments in terms of pH, and oxidation-reduction potentials: Jour. Geology, v. 60, p. 1-33.

Langmuir, D., 1978, Uranium solution-mineral equilibria at low temperatures with applications to sedimentary ore deposits: Geochim. Cosmochin. Acta 42, p. 547-569.

Mauger, R. L., 1981, Geology of the middle part of the Caldera del Nido Block, Chihuahua, Mexico, *in,* P. C. Goodell and A. Waters, eds., Uranium in volcanics and volcaniclastic rocks: AAPG Studies in Geology no. 13, this volume.

McDowell, F., and S. Clabaugh, 1979, Ignimbrites of the Sierra Madre Occidental and their relation to the tectonic history of western Mexico, *in* C. Capin and W. Elston, eds., Ash-flow tuffs: Geol. Soc. America Spec. Paper 180, p. 113-124.

McEldowney, R. C., J. F. Abshier, and D. J. Lootens, 1977, Geology of uranium deposits in the Madison Limestone, Little Mountain area, Big Horn County, Wyoming: Rocky Mtn. Assoc. of Geologists Symp. p. 321-336.

Rankama, K., and T. G. Sahama, 1950, Geochemistry: Chicago, Univ. Chicago Press, 226 p.

Spruill, R. K., 1980, Petrology and geochemistry of peralkaline volcanics of the Sierra Campana, Chihuahua, Mexico (abs.), *in* Abst. with Programs: Southwest Section, AAPG Ann. Mtg., El Paso, p. 56.

Stege, B. R., 1979, Stratigraphy and significance of the carbonates of the Peña Blanca uranium district, Chihuahua, Mexico: unpub. M.S. Thesis, El Paso, Univ. Texas at El Paso, 81 p.

——— N. Pingitore, P. C. Goodell, and D. V. LeMone, 1981, Limestone bedrock geology, Sierra Peña Blanca, Chihuahua, Mexico: this volume.

Tovar, J. C., and J. Valencia, 1974, First-day road log, Ojinaga to Chihuahua City; *in* Geological field trip guidebook through the states of Chihuahua and Sinaloa, Mexico: West Texas Geol. Soc. Pub. 74-63, p. 7-44.

Turekian, K. K. and Wedepohl, 1961, Distribution of the elements in some major units of the earth's crust: Geol. Soc. America Bull., v. 72, p. 175-191.

Waters, A. C., and H. C. Granger, 1953, Volcanic debris in uraniferous sandstones and its possible bearing on the origin and precipitation of uranium: U.S. Geol. Survey Circ. 224, 26 p.

Zielinski, R. A., 1977, Uranium mobility during interaction of rhyolitic glass with alkaline solutions–dissolution of glass: U.S. Geol. Survey Open-File Rept. 77-144, 36 p.

——— 1978, Uranium abundances and distribution in associated glassy and crystalline rhyolites of the western United States: Geol. Soc. America Bull., v. 89, p. 409-414.

——— 1981, Experimental leaching of volcanic glass: Implications for evaluation of glassy volcanic rocks as sources of uranium: this volume.

**Copyright © 1981 by The American Association of Petroleum Geologists.**